



Cite this: *Energy Environ. Sci.*,  
2015, 8, 1719

Received 26th April 2015,  
Accepted 1st May 2015

DOI: 10.1039/c5ee01290b

www.rsc.org/ees

## Electrochemical tuning of olivine-type lithium transition-metal phosphates as efficient water oxidation catalysts†

Yayuan Liu,<sup>a</sup> Haotian Wang,<sup>b</sup> Dingchang Lin,<sup>a</sup> Chong Liu,<sup>a</sup> Po-Chun Hsu,<sup>a</sup> Wei Liu,<sup>a</sup> Wei Chen<sup>a</sup> and Yi Cui<sup>\*ac</sup>

The oxygen evolution reaction is of paramount importance in clean energy generation and storage. While the common approach in search of active, durable and cost-effective oxygen evolution catalysts involves the development of novel materials, it is equally important to tune the properties of existing materials so as to improve their catalytic performance. Here, we demonstrate the general efficacy of electrochemical lithium tuning in organic electrolyte on enhancing the oxygen evolution catalytic activity of olivine-type lithium transition metal phosphates, a widely-researched family of cathode materials in lithium ion batteries. By continuously extracting lithium ions out of lithium transition metal phosphates, the materials exhibited significantly enhanced water oxidation catalytic activity. Particularly, the electrochemically delithiated Li(Ni,Fe)PO<sub>4</sub> nanoparticles anchored on reduced graphene oxide sheets afforded outstanding performance, generating a current density of 10 mA cm<sup>-2</sup> at an overpotential of only 0.27 V for over 24 h without degradation in 0.1 M KOH, outperforming the commercial precious metal Ir catalysts.

The surging global demand for energy, along with the depletion of fossil fuels and the associated adverse environmental impact, has stimulated intense research efforts on sustainable energy conversion and storage systems.<sup>1</sup> A great number of promising energy conversion technologies, such as water electrolyzers, solar fuel synthetic reactors and rechargeable metal-air batteries, are limited by the sluggish kinetics of the oxygen evolution reaction (OER).<sup>2–7</sup> Even with the state-of-the-art catalysts, namely IrO<sub>2</sub> and RuO<sub>2</sub>, a substantial overpotential ( $\eta$ ) is still needed to achieve practical operating current densities ( $\sim 0.3$  V to reach 10 mA cm<sup>-2</sup> current).<sup>8</sup> In addition, the high cost and the scarcity of such precious-metals further impede their implementation on a large scale. Therefore, the importance of developing highly

### Broader context

Water electrolyzers, solar fuel synthetic reactors and rechargeable metal-air batteries are promising technologies to meet the future demand for clean and sustainable energy resources. However, all of these technologies are severely limited by the sluggish kinetics of the oxygen evolution reaction (OER). As a result, the development of highly active, durable water oxidation catalysts that are based on earth-abundant elements is of paramount importance. In the past decade, the research in the area of OER catalysts has been focused on the development of new materials with novel chemistries as well as structures. However, it is equally important to tune the properties of existing materials so as to enhance their catalytic performance. This paper shows that by electrochemically extracting lithium from the well-studied battery materials, the olivine-type lithium transition metal phosphates, their OER performance can be improved dramatically. The demonstrated general efficacy of electrochemical tuning provides an orthogonal method in search for better electrocatalysts.

efficient and durable OER electrocatalysts that are based exclusively on earth-abundant elements can hardly be overemphasized.

Various non-noble metal based OER catalysts have been reported as competitive alternatives, including first-row transition metal oxides and their derivatives,<sup>9–16</sup> perovskites,<sup>17,18</sup> layered double hydroxides,<sup>19–23</sup> carbon-based nonmetal catalysts,<sup>24–26</sup> as well as amorphous Co-phosphate and Ni-borate materials.<sup>27,28</sup> Nevertheless, most of the nonprecious metal catalysts developed so far still underperform the noble metal benchmark. While the continuous search for novel catalytic materials with optimized composition and structure is undoubtedly crucial, it is equally important to controllably tune the properties (such as morphologies, oxidation states, electronic structures and so on) of the existing materials so as to improve their catalytic performance.<sup>20,29–31</sup> Compare to other tuning methods, electrochemical lithium tuning by means of lithium ion intercalation and extraction in battery cells represents a unique, promising tuning strategy, due to the fact that the charge-discharge of a battery cell is a dynamic process that spans a wide potential range. Therefore, by precisely controlling the charge-discharge potential, we can tune the materials in a continuous manner in order to

<sup>a</sup> Department of Materials Science and Engineering, Stanford University, Stanford, CA 94305, USA. E-mail: yicui@stanford.edu

<sup>b</sup> Department of Applied Physics, Stanford University, Stanford, CA 94305, USA

<sup>c</sup> Stanford Institute for Materials and Energy Sciences, SLAC National Accelerator Laboratory, 2575 Sand Hill Road, Menlo Park, California 94025, USA

† Electronic supplementary information (ESI) available. See DOI: 10.1039/c5ee01290b

pinpoint the optimized structures and properties of the catalysts. Our previous studies have demonstrated the effectiveness of electrochemical tuning on improving the electrocatalytic activities of layered materials, such as MoS<sub>2</sub> and LiCoO<sub>2</sub>.<sup>29–31</sup> The success motivates us to wonder whether electrochemical tuning is effective beyond layered structures and can thus be applied to improve the catalytic activities of other battery materials. Since there is a large pool of materials available as battery electrodes, the demonstrated general efficacy of electrochemical tuning could offer a brand new direction to obtain efficient heterogeneous catalysts.

Herein, we demonstrate the general efficacy of electrochemical tuning on olivine-type lithium transition-metal phosphates LiMPO<sub>4</sub> (M = Fe, Mn, Co, Ni) for improved OER performance. While LiMPO<sub>4</sub> compounds have been widely researched as cathode materials for lithium-ion batteries,<sup>32</sup> to the best of our knowledge, there has been no report on them as OER catalysts. By continuously extracting lithium ions out of submicron LiCoPO<sub>4</sub> particles (denoted as LCoP) in organic electrolyte, the material exhibited remarkably enhanced OER performance in alkaline medium. Noticeably, when LiMPO<sub>4</sub> particles were reduced to nanoscale and grown directly on reduced graphene oxide (rGO) sheets, such electrochemical tuning can afford catalysts with unprecedentedly high OER activity that are among the best OER catalysts reported so far. Particularly, the delithiated Li(Ni,Fe)PO<sub>4</sub>/rGO composite (denoted as De-LNiFeP/rGO) showed the best OER performance with an overpotential as low as ~0.274 V to achieve 10 mA cm<sup>-2</sup> current density in 0.1 M KOH and an outstanding long-term stability (10 mA cm<sup>-2</sup> over 24 h without obvious degradation), exceeding the performance of the benchmark Ir-based catalysts.

The electrochemical tuning process is schematically illustrated in Fig. 1. In brief, submicrometer-sized LiMPO<sub>4</sub> particles and LiMPO<sub>4</sub>/rGO composites were synthesized *via* sol-gel and a previously reported two-step approach, respectively.<sup>33,34</sup> The products were then drop casted onto carbon fiber paper substrate (loading 0.5 mg cm<sup>-2</sup>) and assembled into a pouch battery cell configuration acting as the cathode, combined with Li metal as the anode and 1 M LiPF<sub>6</sub> in 1:1 w/w ethylene carbonate/diethyl carbonate as the electrolyte. The electrochemical tuning was carried out by charging the materials to different voltages following the reaction LiMPO<sub>4</sub> → Li<sub>1-x</sub>MPO<sub>4</sub> + xLi<sup>+</sup> + xe<sup>-</sup> (see ESI†).

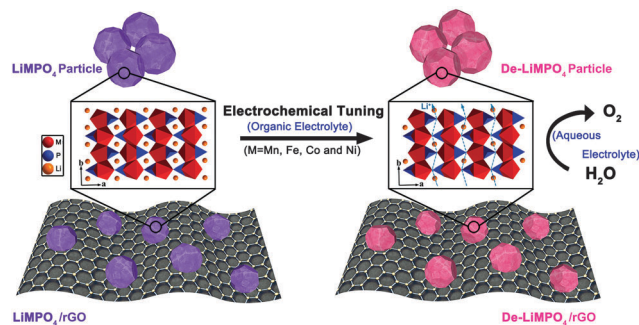


Fig. 1 Schematic illustration of the electrochemical tuning process.

We first study LCoP particles since numerous Co-based materials have been proven to be promising OER catalysts.<sup>12–14,17,18,27</sup> The morphology of LCoP was characterized by scanning electron microscopy (SEM, Fig. 2a), which showed that the particles are of submicrometer size. The X-ray diffraction (XRD) pattern (Fig. S1, ESI†) confirmed the phase purity of LCoP. The OER performance of LCoP before and after electrochemical tuning was investigated in alkaline medium (0.1 M KOH) in a standard three-electrode system (see details in ESI†). The potential required to reach a current density of 10 mA cm<sup>-2</sup> was chosen to compare the performance of the catalysts for the value represents the current density from a device with 12% solar to hydrogen efficiency, which is at the upper end of a realistic device.<sup>2</sup> As can be seen from Fig. 2c, for LCoP before electrochemical tuning, a large  $\eta$  (~550 mV) was needed to reach the current density of 10 mA cm<sup>-2</sup> and the anodic current increased very slowly by applying higher  $\eta$ , indicating the poor OER kinetics of the pristine LCoP. However, when LCoP particles were charged to increasingly higher potentials during electrochemical tuning (denoted as De-LCoP followed by charging voltage), the linear sweep voltammetry (LSV) curves left shifted continuously. Fig. 2d shows the relationship between the average potential at 10 mA cm<sup>-2</sup> and the electrochemical tuning potential in which a pronounced enhancement in OER activity can be observed beyond 4.9 V vs. Li<sup>+</sup>/Li, corresponding to the lithium extraction potential. The best OER performance was obtained by charging LCoP to 5.0 V vs. Li<sup>+</sup>/Li and no significant improvement was seen upon further increasing the charging potential. The saturation in OER performance over 5.0 V could be due to the reason that the material has reached its fully charged state as well as the decomposition of organic electrolyte at elevated potential that blocks the surface active sites. Table 1 summarizes the parameters describing the

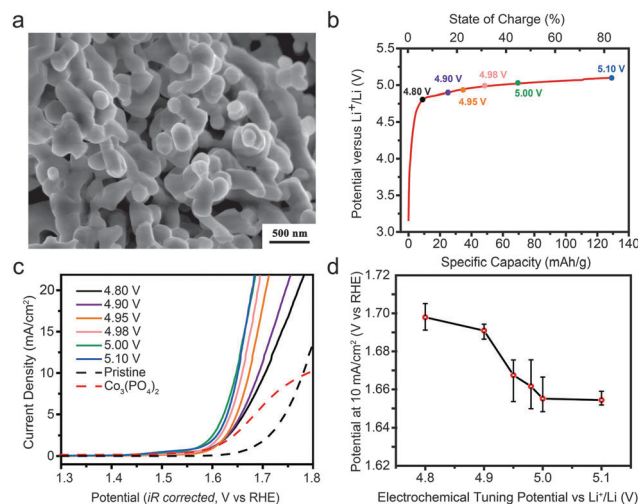


Fig. 2 (a) SEM image of the submicron LCoP particles. (b) A typical charging curve of LCoP. (c) LSV polarization curves (*i*R corrected, vs. reversible hydrogen electrode, RHE) of LCoP charged to different potentials, pristine LCoP and Co<sub>3</sub>(PO<sub>4</sub>)<sub>2</sub> particles in 0.1 M KOH (loading = 0.5 mg cm<sup>-2</sup>). (d) Plots of the electrochemical tuning potentials of LCoP versus the required OER potentials to reach 10 mA cm<sup>-2</sup> current density.

Table 1 Summary of the OER activities of LCoP charged to various potentials

Sample	Average potential at 10 mA cm <sup>-2</sup> (V vs. RHE)	Tafel slopes (mV dec <sup>-1</sup> )	Sample	Average potential at 10 mA cm <sup>-2</sup> (V vs. RHE)	Tafel slopes (mV dec <sup>-1</sup> )
De-LCoP 5.1 V	1.654	77 ± 1	De-LCoP 4.9 V	1.691	73 ± 5
De-LCoP 5.0 V	1.655	52 ± 5	De-LCoP 4.8 V	1.698	83 ± 6
De-LCoP 4.98 V	1.662	67 ± 3	Pristine LCoP	1.781	100 ± 2
De-LCoP 4.95 V	1.668	69 ± 2	Co <sub>3</sub> (PO <sub>4</sub> ) <sub>2</sub>	1.791	109 ± 3

OER performance of the pristine and the delithiated LCoP. Compare to LCoP, the delithiated LCoP above 5.0 V had an almost 130 mV lower  $\eta$  at 10 mA cm<sup>-2</sup>, and the Tafel slope was decreased from  $\sim 100$  mV dec<sup>-1</sup> (pristine LCoP) to  $\sim 52$  mV dec<sup>-1</sup> (De-LCoP 5.0 V). Such a significant improvement confirmed the efficacy of electrochemical tuning on olivine-type LiMPO<sub>4</sub> materials. Notably, delithiated LCoP was also much more active for OER than crystalline Co<sub>3</sub>(PO<sub>4</sub>)<sub>2</sub> particles of similar size (Fig. S2, ESI<sup>†</sup>), indicating that the special olivine structure of the De-LCoP could be accounted for the good OER performance.

It is well-recognized in the battery community that the inherently low ionic and electronic conductivities of LiMPO<sub>4</sub> due to the robust covalent bonding of PO<sub>4</sub><sup>3-</sup> severely limits the charge-discharge kinetics of these materials.<sup>35</sup> Such disadvantages are also believed to be adversely affecting the performance of LiMPO<sub>4</sub> when used as electrocatalysts. In recent years, several strategies have been devised to improve the conductivity and stability of LiMPO<sub>4</sub> in its charged state, including reducing the

particle size to nanoscale, combining the particles with conductive materials such as carbon as well as doping LiMPO<sub>4</sub> with Fe.<sup>36–38</sup> Following the abovementioned rationale, we synthesized LCoP and Fe-doped LiMPO<sub>4</sub> (for higher electronic conductivity) nanoparticles directly anchored on rGO (denoted as LMP/rGO) in seek of even better OER catalyts.

SEM (Fig. 3d inset, Fig. S3, ESI<sup>†</sup>), XRD (Fig. S4, ESI<sup>†</sup>) and energy-dispersive X-ray spectroscopy (EDX, Fig. S5 and Table S1, ESI<sup>†</sup>) were conducted to identify the morphology, phase and composition of the synthesized LMP/rGO hybrid materials respectively. The content of rGO was measured to be approximately 15 wt% *via* thermogravimetric analysis (TGA, Fig. S6, ESI<sup>†</sup>). All the samples were charged to various potentials *vs.* Li<sup>+</sup>/Li during electrochemical tuning (Fig. S7–S11, ESI<sup>†</sup>). Consistent with LCoP, the OER polarization curves shifted to the left for the all samples with increasing tuning potential. Appreciable improvements in OER performance can be observed above 4.80 V (Co<sup>2+/3+</sup>) for LCoP/rGO and LCoFeP/rGO, above 4.30 V (Mn<sup>2+/3+</sup>) for LMnFeP/rGO and

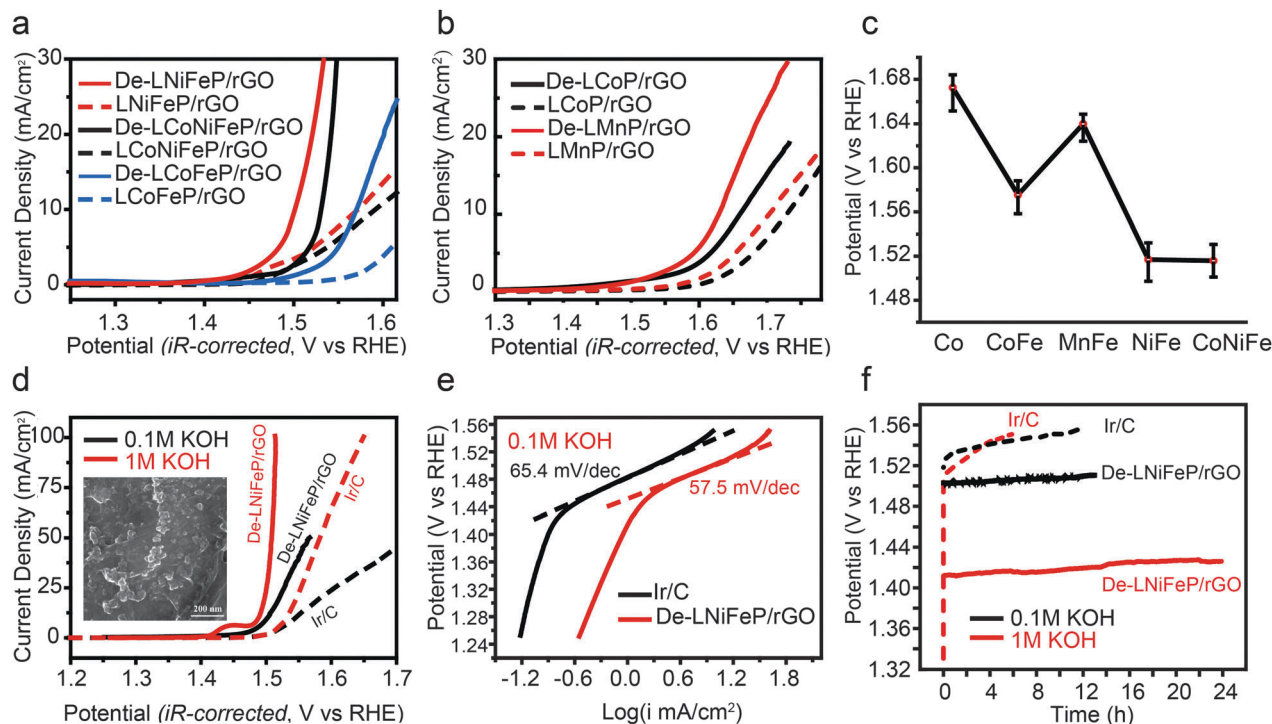


Fig. 3 (a, b) LSV polarization curves of the pristine and delithiated LMP/rGO hybrids in 0.1 M KOH (loading = 0.5 mg cm<sup>-2</sup>). The electrochemical tuning potentials are 5.0 V for De-LCoP/rGO and De-LCoFeP/rGO, 4.5 V for De-LMnFeP/rGO and 5.1 V for De-LNiFeP/rGO and De-LCoNiFeP/rGO. (c) OER potentials at 10 mA cm<sup>-2</sup> current density of the various De-LMP/rGO in 0.1 M KOH (loading = 0.5 mg cm<sup>-2</sup>). (d) LSV polarization curves of De-LNiFeP/rGO and Ir/C in 0.1 and 1 M KOH. The inset is the SEM image of LNiFeP/rGO. (e) Tafel plots of De-LNiFeP/rGO and Ir/C in 0.1 M KOH. (f) Chronopotentiometry curves of De-LNiFeP/rGO and Ir/C at the current density of 10 mA cm<sup>-2</sup> in 0.1 and 1 M KOH.

above 5.00 V ( $\text{Ni}^{2+/3+}$ ) for LNiFeP/rGO, corresponding to the potential of the  $\text{M}^{3+/2+}$  redox couples of the major transition metal elements in these materials.<sup>39</sup> Noticeably, there are two distinct improvement steps for LCoNiFeP/rGO (Fig. S11, ESI<sup>†</sup>), which are above 4.80 V and 5.00 V, corresponding to the redox potential of  $\text{Co}^{2+/3+}$  and  $\text{Ni}^{2+/3+}$  respectively. Fig. 3a and b show the best OER polarization curves of the delithiated LMP/rGO hybrids (denoted as De-LMP/rGO) in comparison with their pristine counterparts. For all the samples, the potential at  $10 \text{ mA cm}^{-2}$  was decreased by around 65–130 mV after the electrochemical tuning process (Fig. S7–S11, ESI<sup>†</sup>), demonstrating the effectiveness of electrochemical tuning on improving the OER performance of olivine-type  $\text{LiMPO}_4$ . Finally, the performance of the De-LMP/rGO hybrids was better than the submicron-sized LCoP, which confirmed that the reduced size, the introduction of Fe and the association with rGO did facilitate the charge transport of  $\text{LiMPO}_4$ .

It can be seen from Fig. 3c that De-LNiFeP/rGO yielded the best OER performance with a potential as low as 1.50 V vs. RHE at  $10 \text{ mA cm}^{-2}$ , which was among the most active non-precious metal OER electrocatalysts (Table S3, ESI<sup>†</sup>). For comparison, a commercial Ir/C catalyst (20 wt% Ir on Vulcan carbon black purchased from Premetek Co.) with the same loading was also tested (Fig. 3d). In 0.1 M KOH, De-LNiFeP/rGO exhibited a lower onset potential ( $\sim 1.45 \text{ V vs. RHE}$ ) than Ir/C ( $\sim 1.50 \text{ V vs. RHE}$ ). In addition, compare to Ir/C, the  $\eta$  of De-LNiFeP/rGO at  $10 \text{ mA cm}^{-2}$  was reduced by 45 mV and the anodic current density increased more rapidly. In 1 M KOH, the onset potential of De-LNiFeP/rGO was reduced to  $\sim 1.47 \text{ V vs. RHE}$ , greatly outperforming that of Ir/C ( $\sim 1.50 \text{ V vs. RHE}$ ). Note that the peak around 1.43 V of De-LNiFeP/rGO in 1 M KOH is attributed to the Ni oxidation process.<sup>40</sup> Moreover, the catalytic kinetics of the two catalysts were examined by Tafel plots (Fig. 3e).

The Tafel slope of De-LNiFeP/rGO is approximately  $57.5 \text{ mV dec}^{-1}$  in 0.1 M KOH, which is lower than that of Ir/C ( $\sim 65.4 \text{ mV dec}^{-1}$ ), suggesting its favorable reaction kinetics. In addition to high OER catalytic activity, De-LNiFeP/rGO also exhibited excellent stability in alkaline solutions (Fig. 3f). When galvanostatically biased at  $10 \text{ mA cm}^{-2}$  in 0.1 M KOH, the catalyst has a nearly constant operating potential for over 13 h ( $\sim 7 \text{ mV}$  increase after 13 h) while the operating potential of Ir/C increased considerably ( $>20 \text{ mV}$ ) after 13 h. In 1 M KOH, De-LNiFeP/rGO operated continuously for 24 h with only  $\sim 14 \text{ mV}$  increase in operating potential, whereas the Ir/C catalyst decayed rapidly within only 6 h ( $\sim 50 \text{ mV}$  increase). These results indicate that LNiFeP/rGO hybrid after electrochemical tuning can afford OER catalysts of high efficiency and durability outperforming the commercial benchmark catalyst.

Various characterizations were carried out to account for the improved OER performance of  $\text{LiMPO}_4$  after electrochemical tuning. First of all, the morphology of the catalysts after delithiation was characterized by SEM (Fig. S12 and S13, ESI<sup>†</sup>), from which no obvious changes can be observed. Therefore, the enhanced catalytic activity was unlikely the result of morphological changes induced by the electrochemical tuning. However, the electrochemically active surface area (ECSA) of the catalysts after tuning increased considerably as estimated from measurements of the electrochemical double-layer capacitance (EDLC). The EDLC of LCoP was only  $\sim 1.25 \text{ mF cm}^{-2}$  whereas that of De-LCoP was  $\sim 11.20 \text{ mF cm}^{-2}$  (Fig. 4a–d), which increased by nearly 10 times after delithiation. Similarly, all the LMP/rGO hybrids after electrochemical tuning exhibited increased EDLC (Fig. S14 and Table S2, ESI<sup>†</sup>) of  $\sim 1.5$ –4 times. The result indicates that the number of electrochemically active sites for water oxidation was increased significantly due to

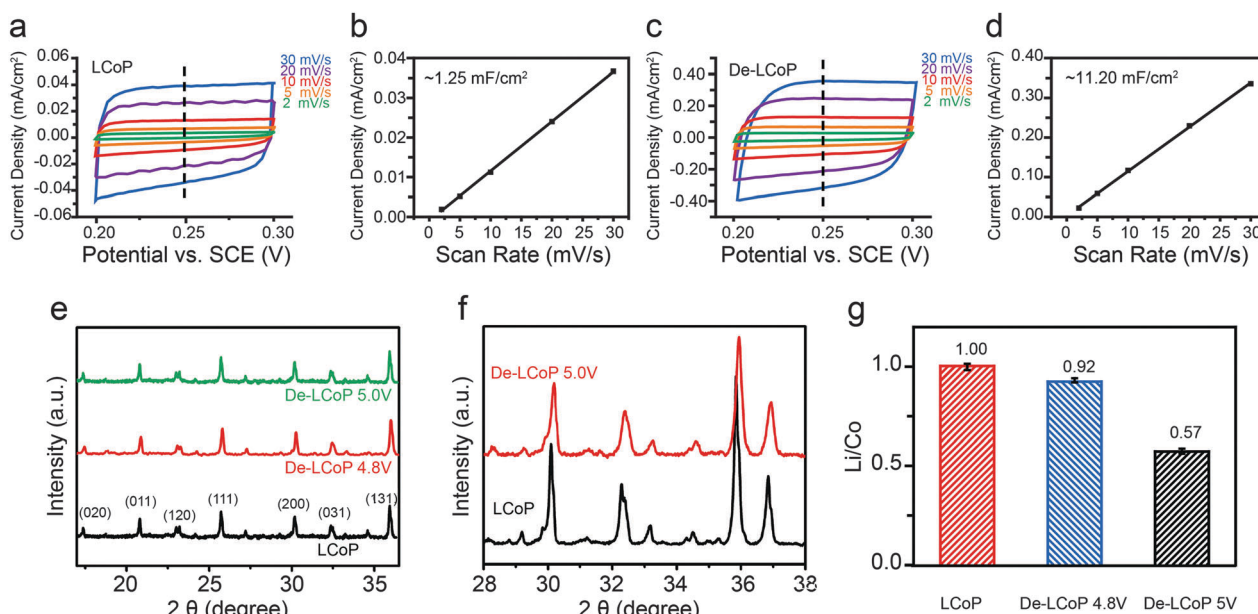


Fig. 4 (a, c) EDLC curves of LCoP and De-LCoP 5.0 V respectively (a with different scan rates; (b, d) plots of current densities at 0.25 V versus scan rates of LCoP and De-LCoP 5.0 V respectively. (e) Powder XRD patterns of LCoP, LCoP 4.8 V and LCoP 5.0 V. (f) Localized XRD patterns of LCoP and LCoP 5.0 V with  $2\theta$  ranging from 28–38°. (g) Li/Co atomic ratio of LCoP, LCoP 4.8 V and LCoP 5.0 V obtained by ICP-MS.

electrochemical tuning, shedding light on the improved OER performance. Noticeably, there exists a positive correlation between the electrochemical tuning potential and the EDLC (Fig. S17, ESI†). With increasing electrochemical tuning potential, the EDLC area of LCoP increases accordingly. The saturation in EDLC above 5.0 V, as mentioned previously, could be attributed to the fact that the material is fully charged as well as the decomposition of the organic electrolyte at high voltage that blocks the active surface sites. Therefore, continuously extracting Li ions will create more active sites for OER. As the increase in EDLC for LCoP is the most significant, it shows the greatest amount of overpotential reduction at 10 mA cm<sup>-2</sup> (126 mV). In addition, as can be observed from the XRD spectra (Fig. 4e), the crystal structure of the olivine-type LiMPO<sub>4</sub> catalysts remained unchanged after electrochemical tuning, which is consistent with existing studies.<sup>41–43</sup> Nevertheless, a slight right-shift of the XRD peaks can be observed due to the shrinking lattices after delithiation (Fig. 4f),<sup>44,45</sup> and the inductively coupled plasma-mass spectroscopy (ICP-MS) analysis further corroborated the extraction of Li<sup>+</sup> by electrochemical tuning (Fig. 4g and Fig. S15, ESI†). Thus, unlike the crystal structures of the previously reported phosphate based OER catalysts and the Co<sub>3</sub>(PO<sub>4</sub>)<sub>2</sub> control in this work,<sup>46,47</sup> such a unique lithium-deficient transition metal phospho-olivine structure that can be obtained only *via* electrochemical route may be responsible for a higher catalytic activity.<sup>48</sup> Moreover, it is believed that the transition metals M (2+) in LiMPO<sub>4</sub> were oxidized for charge compensation when lithium ions were extracted upon electrochemical tuning.<sup>49,50</sup> To confirm the increase in valency, X-ray photoelectron spectroscopy (XPS) was performed on the catalysts before and after delithiation (Fig. S20, ESI†). As can be observed from the spectra, the XPS peaks of the transition metals all shifted to higher binding energy after delithiation, indicating the increased oxidation states of the metal centers. Since transition metal centers of high valency that are capable of buffering the multi-electron processes necessary for water oxidation are generally regarded as catalytically active sites,<sup>51–54</sup> the enhanced OER performance of the delithiated LiMPO<sub>4</sub> is also originated from the increased oxidation state of the metal centers. Finally, in an important study by the Shao-Horn group, a design principle for OER catalysts was established that materials with the most active OER activity shall be the ones with high covalency of transition metal–oxygen bonds.<sup>17</sup> Larger O-2p character of the active M center was reported to promote the surface charge transfer to adsorbates (*e.g.* O<sub>2</sub><sup>2-</sup> and O<sup>2-</sup>), which is the rate determining step in OER. Such principle has been successfully applied to various transition metal OER catalysts systems,<sup>55,56</sup> and we believe is also insightful in explaining the enhanced OER performance of LMP after electrochemical tuning, from a theoretical perspective. From previous studies, delithiation is characterized by the shift of the M-3d bands to lower energies and the increased covalent hybridization between the M-3d and O-2p states.<sup>57</sup> The phenomenon is especially pronounced for delithiated Ni containing LMP,<sup>58</sup> further explaining the notable OER performance of De-LNiFeP/rGO.

In summary, we employed an electrochemical tuning (delithiation) strategy in organic electrolyte to effectively improve the OER performance of olivine-type LiMPO<sub>4</sub> in aqueous solution. Noticeably, the LNiFeP/rGO hybrids upon tuning exhibited unprecedentedly high OER electrocatalytic performance in alkaline solutions, outperforming the commercial Ir/C catalyst in both activity and stability. The improved OER performance could be attributed to the synergistic effect of the increased electrochemically active site density, the higher valency of the transition metal centers and the increased covalent hybridization between the M-3d and O-2p states. The study represents a successful application of electrochemical tuning beyond layered materials and the clearly demonstrated general efficacy of the methodology opens up new venue to fine tune the existing materials for more efficient and durable heterogeneous catalysts in the area of energy research.

## Acknowledgements

This work was initiated by the support of the Department of Energy, Office of Basic Energy Sciences, Materials Sciences and Engineering Division, under contract DE-AC02-76-SFO0515. This work is supported by Global Climate and Energy Project at Stanford University. We acknowledge Professor Matthew W. Kanan and Mr Xiaoquan Min for the help on the gas chromatography measurements.

## Notes and references

- 1 A. S. Arico, P. Bruce, B. Scrosati, J. M. Tarascon and W. Van Schalkwijk, *Nat. Mater.*, 2005, **4**, 366–377.
- 2 C. C. L. McCrory, S. H. Jung, J. C. Peters and T. F. Jaramillo, *J. Am. Chem. Soc.*, 2013, **135**, 16977–16987.
- 3 H. B. Gray, *Nat. Chem.*, 2009, **1**, 7.
- 4 D. G. Nocera, *Acc. Chem. Res.*, 2012, **45**, 767–776.
- 5 C. Liu, J. Y. Tang, H. M. Chen, B. Liu and P. D. Yang, *Nano Lett.*, 2013, **13**, 2989–2992.
- 6 X. M. Ge, Y. Y. Liu, F. W. T. Goh, T. S. A. Hor, Y. Zong, P. Xiao, Z. Zhang, S. H. Lim, B. Li, X. Wang and Z. L. Liu, *ACS Appl. Mater. Interfaces*, 2014, **6**, 12684–12691.
- 7 Y. J. Lin, G. B. Yuan, S. Sheehan, S. Zhou and D. W. Wang, *Energy Environ. Sci.*, 2011, **4**, 4862–4869.
- 8 Y. Lee, J. Suntivich, K. J. May, E. E. Perry and Y. Shao-Horn, *J. Phys. Chem. Lett.*, 2012, **3**, 399–404.
- 9 J. Rosen, G. S. Hutchings and F. Jiao, *J. Am. Chem. Soc.*, 2013, **135**, 4516–4521.
- 10 L. Trotochaud, J. K. Ranney, K. N. Williams and S. W. Boettcher, *J. Am. Chem. Soc.*, 2012, **134**, 17253–17261.
- 11 R. D. L. Smith, M. S. Prevot, R. D. Fagan, Z. P. Zhang, P. A. Sedach, M. K. J. Siu, S. Trudel and C. P. Berlinguette, *Science*, 2013, **340**, 60–63.
- 12 T. Maiyalagan, K. A. Jarvis, S. Therese, P. J. Ferreira and A. Manthiram, *Nat. Commun.*, 2014, **5**, 3949.
- 13 Y. Y. Liang, Y. G. Li, H. L. Wang, J. G. Zhou, J. Wang, T. Regier and H. J. Dai, *Nat. Mater.*, 2011, **10**, 780–786.

- 14 T. Y. Ma, S. Dai, M. Jaroniec and S. Z. Qiao, *J. Am. Chem. Soc.*, 2014, **136**, 13925–13931.
- 15 F. Y. Cheng, J. A. Shen, B. Peng, Y. D. Pan, Z. L. Tao and J. Chen, *Nat. Chem.*, 2011, **3**, 79–84.
- 16 M. R. Gao, Y. F. Xu, J. Jiang, Y. R. Zheng and S. H. Yu, *J. Am. Chem. Soc.*, 2013, **135**, 6378.
- 17 J. Suntivich, K. J. May, H. A. Gasteiger, J. B. Goodenough and Y. Shao-Horn, *Science*, 2011, **334**, 1383–1385.
- 18 Y. Yamada, K. Yano, D. C. Hong and S. Fukuzumi, *Phys. Chem. Chem. Phys.*, 2012, **14**, 5753–5760.
- 19 M. Gong, Y. G. Li, H. L. Wang, Y. Y. Liang, J. Z. Wu, J. G. Zhou, J. Wang, T. Regier, F. Wei and H. J. Dai, *J. Am. Chem. Soc.*, 2013, **135**, 8452–8455.
- 20 F. Song and X. L. Hu, *Nat. Commun.*, 2014, **5**, 4477.
- 21 X. Long, S. Xiao, Z. L. Wang, X. L. Zheng and S. H. Yang, *Chem. Commun.*, 2015, **51**, 1120–1123.
- 22 X. Long, J. K. Li, S. Xiao, K. Y. Yan, Z. L. Wang, H. N. Chen and S. H. Yang, *Angew. Chem., Int. Ed.*, 2014, **53**, 7584–7588.
- 23 B. M. Hunter, J. D. Blakemore, M. Deimund, H. B. Gray, J. R. Winkler and A. M. Muller, *J. Am. Chem. Soc.*, 2014, **136**, 13118–13121.
- 24 G. L. Tian, M. Q. Zhao, D. S. Yu, X. Y. Kong, J. Q. Huang, Q. Zhang and F. Wei, *Small*, 2014, **10**, 2251–2259.
- 25 Y. Zhao, R. Nakamura, K. Kamiya, S. Nakanishi and K. Hashimoto, *Nat. Commun.*, 2013, **4**, 2390.
- 26 H. W. Park, D. U. Lee, Y. L. Liu, J. S. Wu, L. F. Nazar and Z. W. Chen, *J. Electrochem. Soc.*, 2013, **160**, A2244–A2250.
- 27 M. W. Kanan and D. G. Nocera, *Science*, 2008, **321**, 1072–1075.
- 28 M. Dinca, Y. Surendranath and D. G. Nocera, *Proc. Natl. Acad. Sci. U. S. A.*, 2010, **107**, 10337–10341.
- 29 H. T. Wang, Z. Y. Lu, S. C. Xu, D. S. Kong, J. J. Cha, G. Y. Zheng, P. C. Hsu, K. Yan, D. Bradshaw, F. B. Prinz and Y. Cui, *Proc. Natl. Acad. Sci. U. S. A.*, 2013, **110**, 19701–19706.
- 30 H. T. Wang, Z. Y. Lu, D. S. Kong, J. Sun, T. M. Hymel and Y. Cui, *ACS Nano*, 2014, **8**, 4940–4947.
- 31 Z. Y. Lu, H. T. Wang, D. S. Kong, K. Yan, P. C. Hsu, G. Y. Zheng, H. B. Yao, Z. Liang, X. M. Sun and Y. Cui, *Nat. Commun.*, 2014, **5**, 4345.
- 32 M. S. Whittingham, *Chem. Rev.*, 2004, **104**, 4271–4301.
- 33 E. J. Kim, H. Y. Xu, J. S. Lim, J. W. Kang, J. H. Gim, V. Mathew and J. Kim, *J. Solid State Electrochem.*, 2012, **16**, 149–155.
- 34 H. L. Wang, Y. Yang, Y. Y. Liang, L. F. Cui, H. S. Casalongue, Y. G. Li, G. S. Hong, Y. Cui and H. J. Dai, *Angew. Chem., Int. Ed.*, 2011, **50**, 7364–7368.
- 35 A. Yamada, M. Hosoya, S. C. Chung, Y. Kudo, K. Hinokuma, K. Y. Liu and Y. Nishi, *J. Power Sources*, 2003, **119**, 232–238.
- 36 X. H. Rui, X. X. Zhao, Z. Y. Lu, H. T. Tan, D. H. Sim, H. H. Hng, R. Yazami, T. M. Lim and Q. Y. Yan, *ACS Nano*, 2013, **7**, 5637–5646.
- 37 S. M. Oh, S. W. Oh, C. S. Yoon, B. Scrosati, K. Amine and Y. K. Sun, *Adv. Funct. Mater.*, 2010, **20**, 3260–3265.
- 38 S. K. Martha, J. Grinblat, O. Haik, E. Zinigrad, T. Drezen, J. H. Miners, I. Exnar, A. Kay, B. Markovsky and D. Aurbach, *Angew. Chem., Int. Ed.*, 2009, **48**, 8559–8563.
- 39 J. Molenda, A. Kulka, A. Milewska, W. Zajac and K. Swierczek, *Materials*, 2013, **6**, 1656–1687.
- 40 D. A. Corrigan and S. L. Knight, *J. Electrochem. Soc.*, 1989, **136**, 613–619.
- 41 M. Nakayama, S. Goto, Y. Uchimoto, M. Wakihara and Y. Kitajima, *Chem. Mater.*, 2004, **16**, 3399–3401.
- 42 M. S. Whittingham, *Chem. Rev.*, 2014, **114**, 11414–11443.
- 43 Q. D. Truong, M. K. Deyaraju, Y. Sasaki, H. Hyodo, T. Tomai and I. Honma, *Chem. Mater.*, 2014, **26**, 2770–2773.
- 44 H. Ju, J. Wu and Y. Xu, *Int. J. Energy Environ. Eng.*, 2013, **4**, 1–6.
- 45 N. N. Bramnik, K. G. Bramnik, C. Baetz and H. Ehrenberg, *J. Power Sources*, 2005, **145**, 74–81.
- 46 J. C. Zhang, Y. Yang, Z. C. Zhang, X. B. Xu and X. Wang, *J. Mater. Chem. A*, 2014, **2**, 20182–20188.
- 47 K. Jin, J. Park, J. Lee, K. D. Yang, G. K. Pradhan, U. Sim, D. Jeong, H. L. Jang, S. Park, D. Kim, N. E. Sung, S. H. Kim, S. Han and K. T. Nam, *J. Am. Chem. Soc.*, 2014, **136**, 7435–7443.
- 48 H. Ehrenberg, N. N. Bramnik, A. Senyshyn and H. Fuess, *Solid State Sci.*, 2009, **11**, 18–23.
- 49 M. Kaus, I. Issac, R. Heinzmann, S. Doyle, S. Mangold, H. Hahn, V. S. K. Chakravadhanula, C. Kubel, H. Ehrenberg and S. Indris, *J. Phys. Chem. C*, 2014, **118**, 17279–17290.
- 50 I. Bezza, M. Kaus, R. Heinzmann, M. Yavuz, M. Knapp, S. Mangold, S. Doyle, C. P. Grey, H. Ehrenberg, S. Indris and I. Saadoun, *J. Phys. Chem. C*, 2015, **119**, 9016–9024.
- 51 J. G. McAlpin, Y. Surendranath, M. Dinca, T. A. Stich, S. A. Stojan, W. H. Casey, D. G. Nocera and R. D. Britt, *J. Am. Chem. Soc.*, 2010, **132**, 6882–6883.
- 52 S. C. Ma, L. Q. Sun, L. N. Cong, X. G. Gao, C. Yao, X. Guo, L. H. Tai, P. Mei, Y. P. Zeng, H. M. Xie and R. S. Wang, *J. Phys. Chem. C*, 2013, **117**, 25890–25897.
- 53 J. B. Gerken, S. E. Shaner, R. C. Masse, N. J. Porubsky and S. S. Stahl, *Energy Environ. Sci.*, 2014, **7**, 2376–2382.
- 54 Y. F. Sun, S. Gao, F. C. Lei, J. W. Liu, L. Liang and Y. Xie, *Chem. Sci.*, 2014, **5**, 3976–3982.
- 55 Y. W. Liu, H. Cheng, M. J. Lyu, S. J. Fan, Q. H. Liu, W. S. Zhang, Y. D. Zhi, C. M. Wang, C. Xiao, S. Q. Wei, B. J. Ye and Y. Xie, *J. Am. Chem. Soc.*, 2014, **136**, 15670–15675.
- 56 U. Maitra, B. S. Naidu, A. Govindaraj and C. N. Rao, *Proc. Natl. Acad. Sci. U. S. A.*, 2013, **110**, 11704–11707.
- 57 M. K. Kinyanjui, P. Axmann, M. Wohlfahrt-Mehrens, P. Moreau, F. Boucher and U. Kaiser, *J. Phys.: Condens. Matter*, 2010, **22**, 2775501.
- 58 A. Bhowmik, T. Sarkar, A. K. Varanasi, U. V. Waghmare and M. D. Bharadwaj, *J. Renewable Sustainable Energy*, 2013, **5**, 053130.